Electronic Supporting Information

Temperature Sensing of $Sr_3Y_2Ge_3O_{12}:Bi^{3+},Sm^{3+}$ Garnet Phosphors with Tunable Sensitivity

Rui Sun,[a,b] Xiang Wei,[a] Huijuan Yu,*[a] Pengyun Chen,[b] Haiyong Ni,[b] Junhao Li,[b] Jiansheng Huo,[b] Jianbang Zhou*[b] and Qiuhong Zhang*[b]

[a] School of Chemical Engineering and Light Industry, Guangdong University of Technology, Guangzhou 510006, PR China

[b] Key Laboratory of Separation and Comprehensive Utilization of Rare Metals, Guangdong Province Key Laboratory of Rare Earth Development and Application, Institute of Resources Utilization and Rare Earth Development, Guangdong Academy of Sciences, Guangzhou 510651, PR China

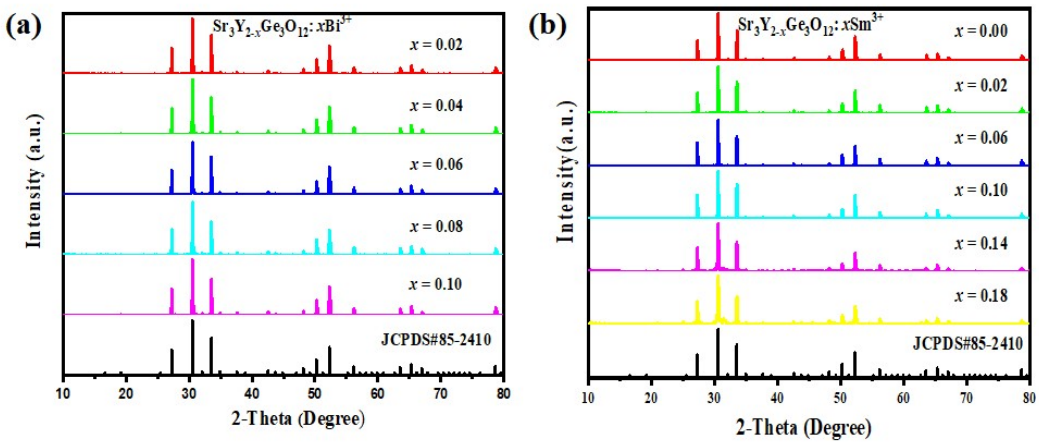

Fig. S1 The XRD patterns of (a) $Sr_3Y_2Ge_3O_{12}$:yBi^{3+} (y = 0.02 - 0.10) and (b) $Sr_3Y_2Ge_3O_{12}$:xSm^{3+} (x = 0.02 - 0.18).

The XRD patterns of $Sr_3Y_2Ge_3O_{12}$:yBi^{3+} (y = 0.02 - 0.10) and $Sr_3Y_2Ge_3O_{12}$:xSm^{3+} (x = 0.02 - 0.18) are shown in **Fig. S1a** and **S1b**. It could be observed that the diffraction peaks $Sr_3Y_2Ge_3O_{12}$:yBi^{3+} (y = 0.02 - 0.10) matched well with the standard diffraction pattern of $Sr_3Y_2Ge_3O_{12}$ (JCPDS 85-2410). When the doping Sm^{3+} concentration is $x \geq 0.14$, the impurity appears in the $Sr_3Y_2Ge_3O_{12}$:xSm^{3+} (x = 0.02 - 0.18) sample.

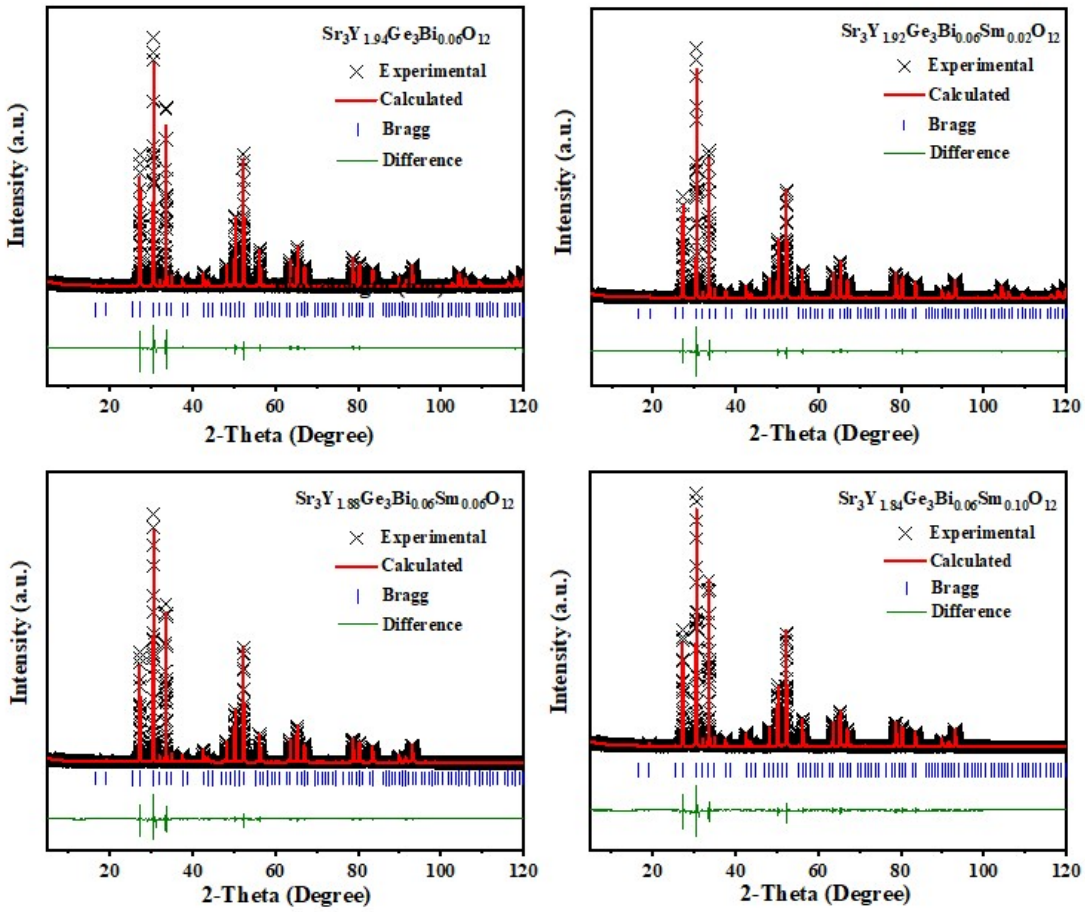

Fig. S2 XRD Rietveld refinement of $Sr_3Y_2Ge_3O_{12}$:0.06Bi^{3+},xSm^{3+}(x = 0 - 0.10).

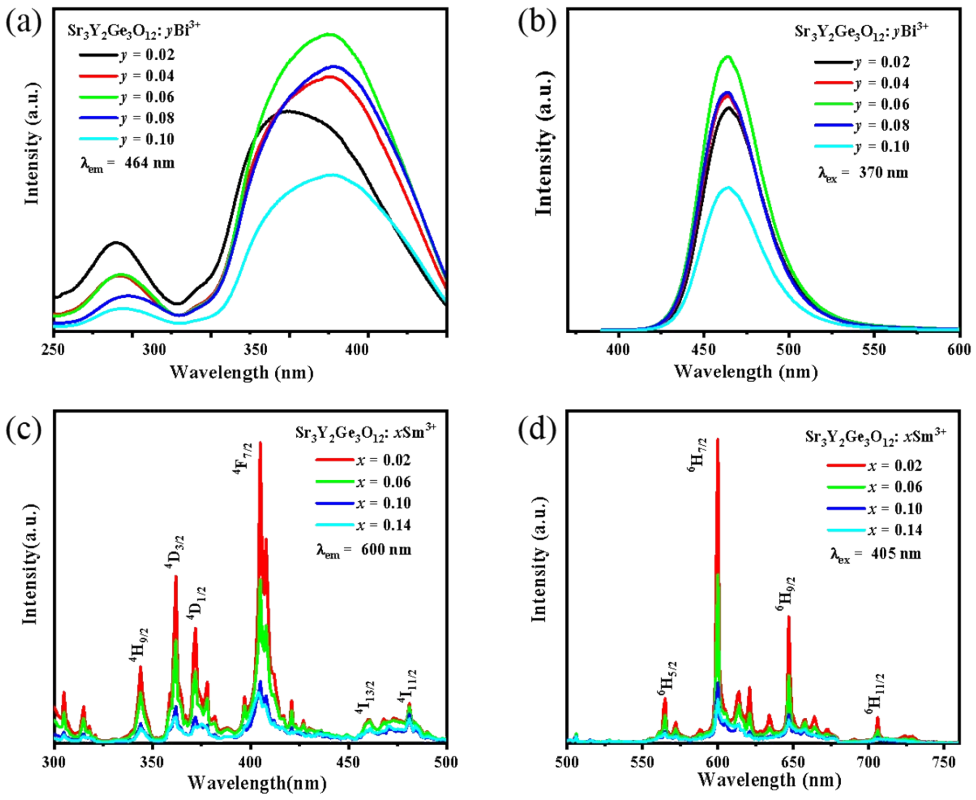

Fig. S3 The PLE (a) and PL (b) spectrum of $Sr_3Y_2Ge_3O_{12}$:$y$$Bi^{3+}$ (y = 0.02 - 0.10), The PLE (c) and PL (d) spectrum of $Sr_3Y_2Ge_3O_{12}$:$x$$Sm^{3+}$ (x = 0.02 - 0.14).

The intensity of both the PLE and PL spectra of $Sr_3Y_2Ge_3O_{12}$: $y$$Bi^{3+}$($y$ = 0.02 - 0.10) increased firstly with increasing content and reached the maximum at y = 0.06, then decreased due to concentration quenching. Similarly, the $Sr_3Y_2Ge_3O_{12}$: $x$$Sm^{3+}$($x$ = 0.02 - 0.14) showed an optimal concentration at x = 0.02.

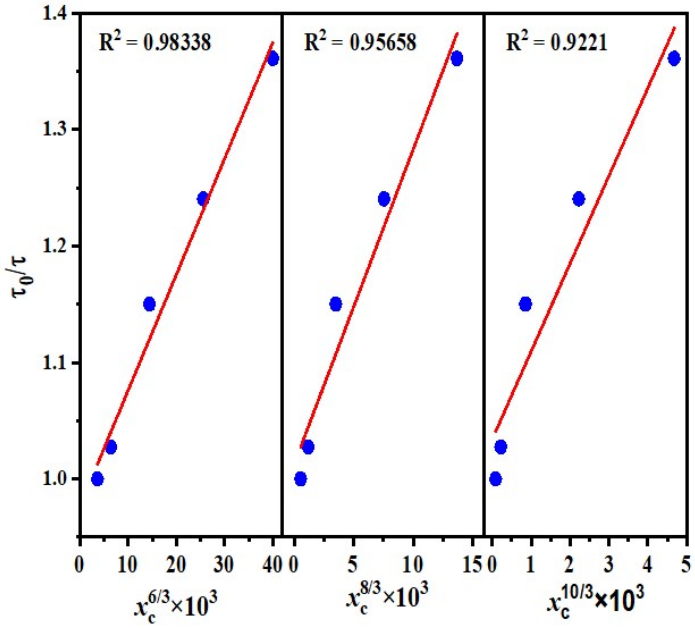

Fig. S4 Dependence of τ_0/τ on $C^{6/3}$, $C^{8/3}$, and $C^{10/3}$.

In general, the energy transfer between sensitizer and activator in the host may occur via two main mechanisms, namely exchange interaction and electric multipolar interaction. To verify which of these mechanisms plays an important role, the critical distance *Rc* between Bi^{3+} and Sm^{3+} in $Sr_3Y_2Ge_3O_{12}$ was estimated using the following equation:

$$R_C = 2 \times [\frac{3V}{4\pi\chi_C \mathrm{N}}]^{1/3}$$

where *V* corresponds to the volume of the unit cell, *N* is the number of host cations in the unit cell, and *Xc* is the critical total concentration of Bi^{3+} and Sm^{3+}. For $Sr_3Y_2Ge_3O_{12}$:0.06Bi^{3+}, 0.018Sm^{3+} phosphor, $N = 8$, $V = 2241.46$ Å^3, $\chi = 0.06+0.018 = 0.078$, the *Rc* between Bi^{3+} and Sm^{3+} was calculated to be 19.00 Å. Thus, in the case of the maximum doping concentration, it still exceeds a distance of 8, excluding the possibility of exchange interactions. The energy transfer from Bi^{3+} to Sm^{3+} mainly resulted from multipolar interactions.

To further investigate the specific energy transfer mechanism between the sensitizer Bi^{3+} and the activator Sm^{3+} in $Sr_3Y_2Ge_3O_{12}$, we used Dexter energy transfer theory for a deeper elaboration. Dexter energy transfer theory and Reisfeld's approximation are expressed as follows:

$$\frac{\tau_0}{\tau} \propto C^{n/3}$$

where C is the sum of Bi^{3+} and Sm^{3+} concentration in the sample; and n is a constant. Different values of n values indicate different interaction models, which correspond to dipole-dipole (d-d) interaction, dipole-quadrupole (d-q) interaction and quadrupole-quadrupole (q-q) interaction when n = 6, 8 and 10, respectively. The linear fit between τ_0/τ and the total concentration C for different values of n are depicted in **Fig. S4**. It was clearly that the best linear fit was achieved when n = 6, which indicated that the energy transfer mechanism between Bi^{3+} and Sm^{3+} was mainly dipole-dipole interaction.

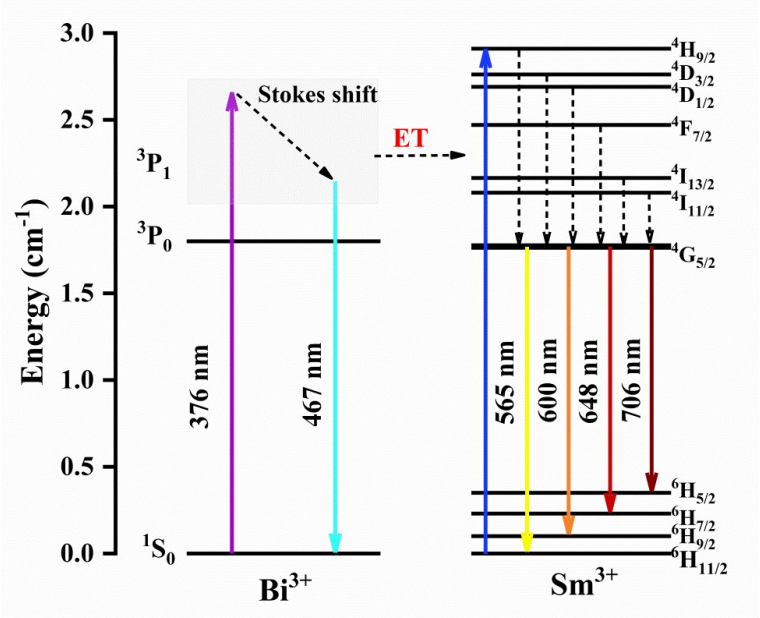

Fig. S5 The energy level diagrams of Bi^{3+} and Sm^{3+} ions in $Sr_3Y_2Ge_3O_{12}$.

The energy level diagrams of Bi^{3+} and Sm^{3+} ions in $Sr_3Y_2Ge_3O_{12}$ are present in **Fig. S5** to explain the energy transfer process in detail. The free electrons of the Bi^{3+} ions can absorb UV light and jump from the $^1S_0$ ground state to the $^3P_1$ excited state. On the one hand, part of the excited electrons falls back to the ground $^1S_0$ state and gives out a broad blue emission band of in the range of 420 – 540 nm. On the other hand, some of the excited electrons migrate to neighboring Sm^{3+} ions, and then relax radiatively from $^4G_{5/2}$ excited state to the lower $^6H_{11/2}$, $^6H_{9/2}$, $^6H_{7/2}$ and $^6H_{5/2}$ states, producing the typical emission at 565, 600, 648 and 706 nm, respectively. Meanwhile,

the free electrons of Sm^{3+} can also absorb UV light and jump to the excited state, and then gives its characteristic f-f emissions as mentioned above.

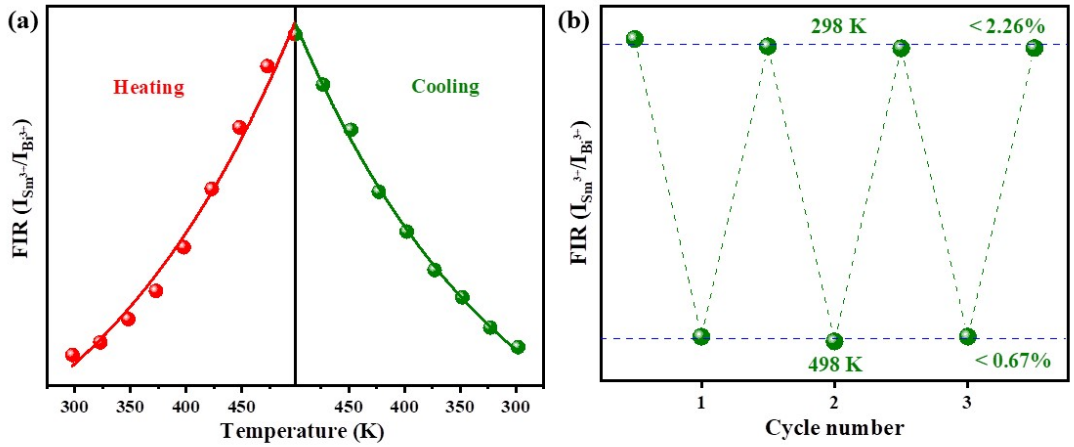

Fig. S6 (a) Temperature-dependent FIR (I_{Sm}^{3+}/I_{Bi}^{3+}) of $Sr_3Y_2Ge_3O_{12}$:0.06Bi^{3+},0.02Sm^{3+} phosphor upon the cycling process of heating and cooling in the temperature range from 298 to 498 K. (b) Temperature cycling of FIR in the temperature 298-498 K.

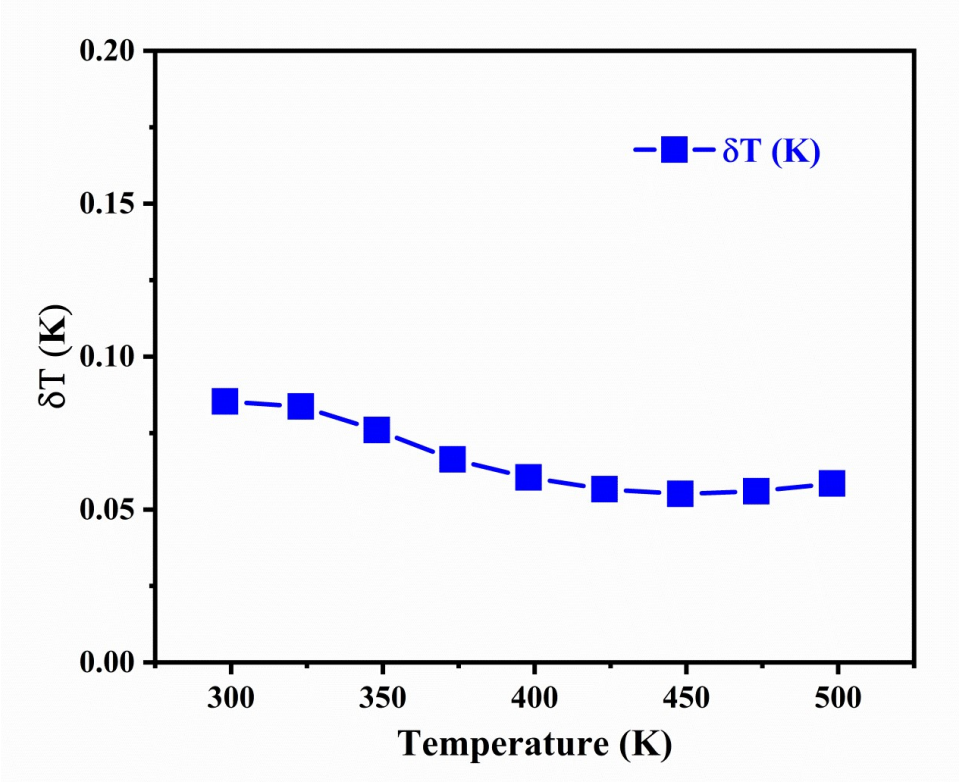

Fig. S7 The temperature resolution of $Sr_3Y_2Ge_3O_{12}$:0.06Bi^{3+},0.02Sm^{3+} phosphor in the range of 298-498 K.

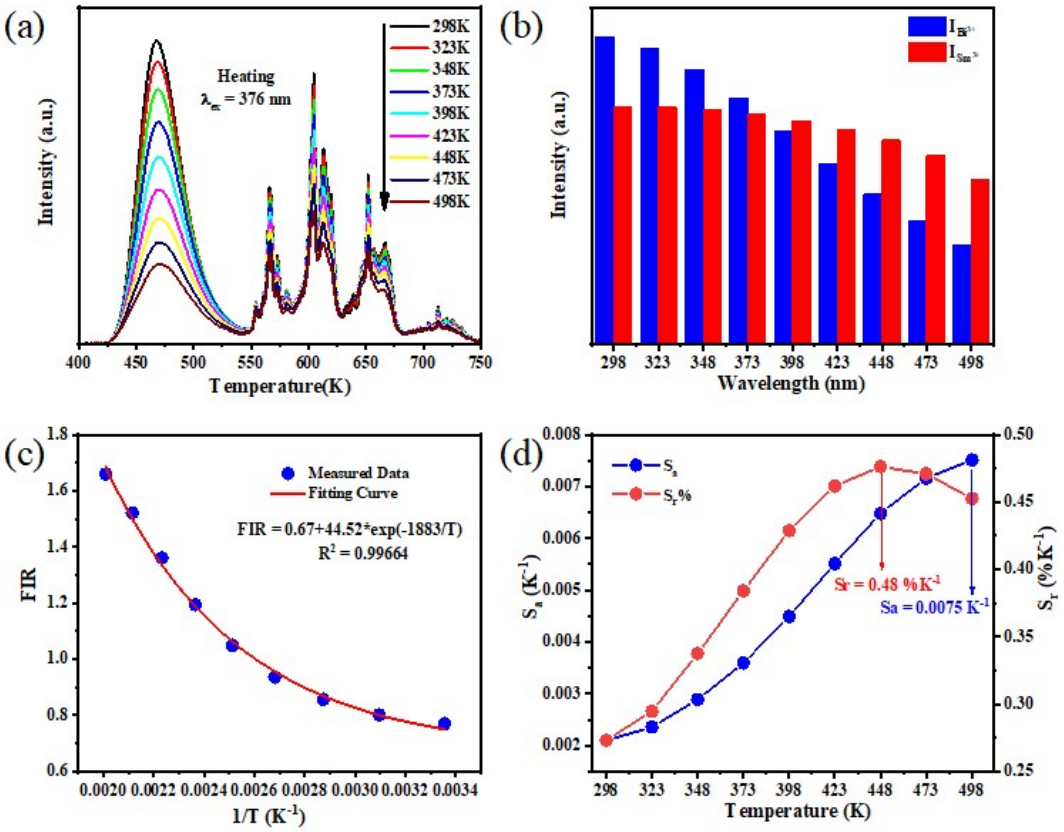

Fig. S8 (a) Emission spectra of $Sr_3Y_2Ge_3O_{12}$:0.06Bi^{3+},0.06Sm^{3+} from 298 to 498 K, (b) The integrated PL intensity of Bi^{3+} and Sm^{3+} from 298 K to 498 K, (c) Measured and fitted FIR data of $Sr_3Y_2Ge_3O_{12}$:0.06Bi^{3+},0.06Sm^{3+}, (d) Dependence of S_a and S_r on T.

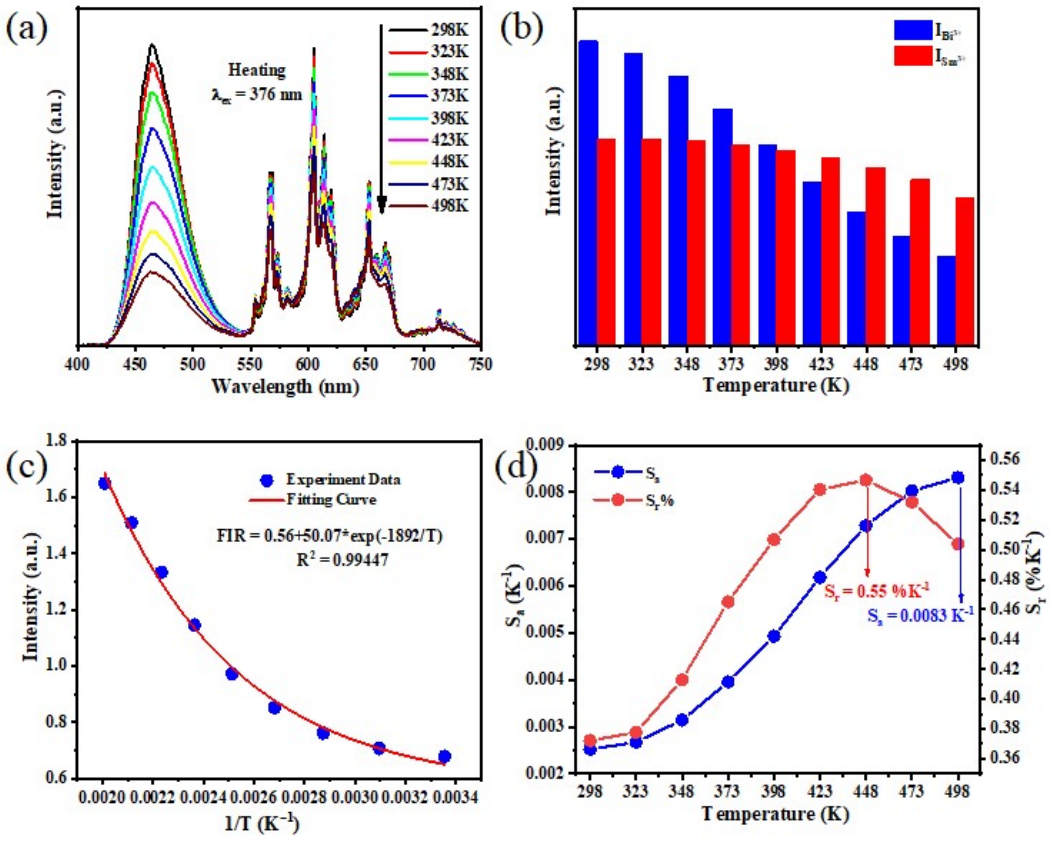

Fig. S9 (a) Emission spectra of $Sr_3Y_2Ge_3O_{12}$:0.06Bi^{3+},0.10Sm^{3+} from 298 to 498 K, (b) The integrated PL intensity of Bi^{3+} and Sm^{3+} from 298 K to 498 K, (c) Measured and fitted FIR data of $Sr_3Y_2Ge_3O_{12}$:0.06Bi^{3+},0.10Sm^{3+}, (d) Dependence of S_a and S_r on T.

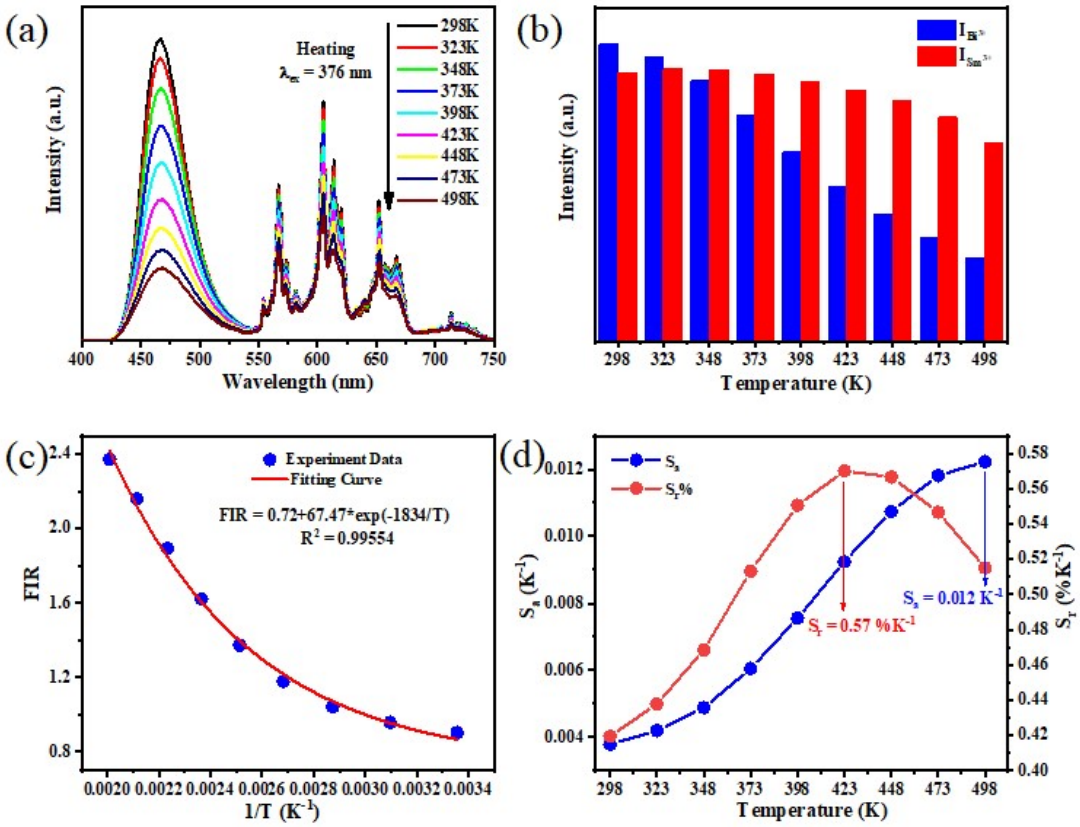

Fig. S10 (a) Emission spectra of $Sr_3Y_2Ge_3O_{12}$:0.06Bi^{3+},0.14Sm^{3+} from 298 to 498 K, (b) The integrated PL intensity of Bi^{3+} and Sm^{3+} from 298 K to 498 K, (c) Measured and fitted FIR data of $Sr_3Y_2Ge_3O_{12}$:0.06Bi^{3+},0.14Sm^{3+}, (d) Dependence of S_a and S_r on T.

Table S1 Rietveld refinement and crystallographic data of $Sr_3Y_{1.94}Bi_{0.06}Ge_3O_{12}$.

Formula	$Sr_3Y_{1.94}Bi_{0.06}Ge_3O_{12}$
Crystal system	Cubic
Space group	$Ia\bar{3}d$ (230, O_h^{10})
Cell Parameters	a= 13.08235 Å
Cell Parameters Volume	V= 2239.016 Å^3
Reliability factors	R_{wp}= 15.83%, R_p= 11.08 % and GOF= 2.99

Atom	Site	x	y	z	Occupancy	U_{iso}
Sr^{2+}	24c	0.125	0.00	0.25	1	0.024
Y^{3+}/Bi^{3+}	16a	0.00	0.00	0.00	1	0.022
Ge^{4+}	24d	0.375	0	0.25	1	0.021
O^{2-}	96h	0.965	0.054	0.160	1	0.029

Table S2 Rietveld refinement and crystallographic data of $Sr_3Y_{1.92}Bi_{0.06}Sm_{0.02}Ge_3O_{12}$.

Formula	$Sr_3Y_{1.92}Bi_{0.06}Sm_{0.02}Ge_3O_{12}$
Crystal system	Cubic
Space group	$Ia\bar{3}d$ (230, O_h^{10})
Cell Parameters	a= 13.08323 Å
Cell Parameters Volume	V= 2239.468 Å^3
Reliability factors	R_{wp}= 15.42%, R_p= 10.11 % and GOF= 2.83

Atom	Site	x	y	z	Occupancy	U_{iso}
Sr^{2+}	24c	0.125	0.00	0.25	1	0.025
$Y^{3+}/Bi^{3+}/Sm^{3+}$	16a	0.00	0.00	0.00	1	0.025
Ge^{4+}	24d	0.375	0	0.25	1	0.021
O^{2-}	96h	0.959	0.051	0.158	1	0.027

Table S3 Rietveld refinement and crystallographic data of $Sr_3Y_{1.88}Bi_{0.06}Sm_{0.06}Ge_3O_{12}$.

Formula	$Sr_3Y_{1.88}Bi_{0.06}Sm_{0.06}Ge_3O_{12}$
Crystal system	Cubic
Space group	$Ia\bar{3}d$ (230, O_h^{10})
Cell Parameters	a= 13.08423 Å
Cell Parameters Volume	V= 2239.982 Å^3
Reliability factors	R_{wp}= 15.26%, R_p= 9.52 % and GOF= 2.80

Atom	Site	x	y	z	Occupancy	U_{iso}
Sr^{2+}	24c	0.125	0.00	0.25	1	0.027
$Y^{3+}/Bi^{3+}/Sm^{3+}$	16a	0.00	0.00	0.00	1	0.025
Ge^{4+}	24d	0.375	0	0.25	1	0.025
O^{2-}	96h	0.959	0.051	0.159	1	0.029

Table S4 Rietveld refinement and crystallographic data of $Sr_3Y_{1.84}Bi_{0.06}Sm_{0.10}Ge_3O_{12}$.

Formula	$Sr_3Y_{1.84}Bi_{0.06}Sm_{0.10}Ge_3O_{12}$
Crystal system	Cubic
Space group	$Ia\bar{3}d$ (230, O_h^{10})
Cell Parameters	a= 13.0875 Å
Cell Parameters Volume	V= 2241.662 Å^3
Reliability factors	R_{wp}= 14.26%, R_p= 9.28 % and GOF= 2.60

Atom	Site	x	y	z	Occupancy	U_{iso}
Sr^{2+}	24c	0.125	0.00	0.25	1	0.030
$Y^{3+}/Bi^{3+}/Sm^{3+}$	16a	0.00	0.00	0.00	1	0.027
Ge^{4+}	24d	0.375	0	0.25	1	0.028
O^{2-}	96h	0.960	0.054	0.158	1	0.033

Table S5 Rietveld refinement and crystallographic data of $Sr_3Y_{1.8}Bi_{0.06}Sm_{0.14}Ge_3O_{12}$.

Formula	$Sr_3Y_{1.8}Bi_{0.06}Sm_{0.14}Ge_3O_{12}$
Crystal system	Cubic
Space group	$Ia\bar{3}d$ (230, O_h^{10})
Cell Parameters	a= 13.08755 Å
Cell Parameters Volume	V= 2241.687 Å^3
Reliability factors	R_{wp}= 11.55%, R_p= 7.58 % and GOF= 2.11

Atom	Site	x	y	z	Occupancy	U_{iso}
Sr^{2+}	24c	0.125	0.00	0.25	1	0.034
$Y^{3+}/Bi^{3+}/Sm^{3+}$	16a	0.00	0.00	0.00	1	0.030
Ge^{4+}	24d	0.375	0	0.25	1	0.031
O^{2-}	96h	0.958	0.051	0.158	1	0.041

Table S6 Relative sensitivities (S_r) of some garnet FIR type thermometers.

Compounds	Temperature (K)	S_r (%K^{-1})	Ref.
$Sr_3Y_2Ge_3O_{12}:Bi^{3+},Sm^{3+}$	298-498 K	0.61	This work
YAG:Nd^{3+}	283-342 K	0.15	[21]
GGG:Yb,Er	300-973 K	0.41	[22]
$Ca_2YZr_2Al_3O_{12}:Bi^{3+},Eu^{3+}$	250-575 K	0.664	[23]
$Li_3Gd_3Te_2O_{12}:Bi^{3+}$, Pr^{3+}	100-300 K	0.672	[24]
LuAG:Eu^{3+}/Mn^{4+}	303-358 K	0.7	[25]
$Mg_3Y_2Ge_3O_{12}:Ce^{3+}$, Cr^{3+}	298-573 K	1.38	[26]
$Sr_2NaMg_2V_3O_{12}:Eu^{3+}$	300-500 K	1.61	[27]
LuAG:Ce^{3+},Mn^{4+}	100-350 K	4.37	[28]